Food and Chemical Toxicology 134 (2019) 110861

Contents lists available at ScienceDirect

Food and Chemical Toxicology

journal homepage: www.elsevier.com/locate/foodchemtox

Apoptosis effect of *Aegiceras corniculatum* on human colorectal cancer via activation of FoxO signaling pathway

Hua Luo[a,b,e,1], Erwei Hao[a,b,1], Dechao Tan[a,b], Wei Wei[a,b], Jinling Xie[a,b], Xiaohui Feng[a,b], Zhengcai Du[a,b], Chunying Huang[a,b], Gang Bai[d], Yuanyuan Hou[d], Chuanjing Cheng[d], Xiangxi Yi[a,b], Yitao Wang[e], Xiaotao Hou[a,b,c,**], Jiagang Deng[a,b,*]

[a] Guangxi Key Laboratory of Efficacy Study on Chinese Materia Medica, Guangxi University of Chinese Medicine, Nanning, China
[b] Guangxi Collaborative Innovation Center for Research on Functional Ingredients of Agricultural Residues, Guangxi University of Chinese Medicine, Nanning, China
[c] Faculty of Pharmacy, Guangxi University of Chinese Medicine, Nanning, China
[d] College of Pharmacy, Nankai University, Tianjing, China
[e] Institute of Chinese Medical Sciences, State Key Laboratory of Quality Research in Chinese Medicine, University of Macau, MO, China

ARTICLE INFO

Keywords:
Forkhead box
Aegiceras corniculatum
Colorectal cancer
Apoptosis
Cell cycle

ABSTRACT

Aegiceras corniculatum (L.) Blanco is known to exhibit anticancer effects against different types of cancer; however, to the best of our knowledge, the anticancer activity and underlying mechanisms of action of *A. corniculatum* leaf extract on colorectal cancer have not been elucidated. In the present study, colony-forming assay, western blot analysis, flow cytometry, and a xenograft model were used to investigate the effects of an *n*-butanol extract of *A. corniculatum* leaves (NACL) on colorectal cancer *in vitro* and *in vivo*. The results showed that NACL inhibits the viability and proliferation of colorectal cancer cells in a dose-dependent manner. Besides, NACL also induces cell apoptosis and cell cycle arrest by activating Forkhead box proteins and controlling the cell cycle checkpoint pathways, which are associated with the caspase-dependent mitochondrial apoptotic cascades and Bcl-2 family proteins. More importantly, the tumour sizes in HT-29 xenograft nude mice decreased after treatment with NACL *in vivo*. These findings indicate that *A. corniculatum* leaf extracts have potent anticancer activities across different colorectal and other solid tumour cell lines, via regulation of the cell cycle and apoptosis; thus, it has the potential to be developed as an anticancer agent to enhance clinical standards of care for patients with colorectal cancer.

1. Introduction

Colorectal cancer is one of the most common malignancies worldwide and is the second leading cause of cancer-related death. It is more prevalent in China and other Asian countries, with an estimated 1.4 million new cases and more than 0.7 million deaths in 2013 (Alkema et al., 2016; Chen et al., 2016; Kuipers et al., 2015; Siegel et al., 2017a, 2017b; Torre et al., 2015). Surgical resection followed by adjuvant chemotherapy or radiotherapy is regarded as the first choice of treatment for patients with colorectal cancer; however, 30%–50% of patients who underwent curative resection experience local and systemic recurrence. Locoregional relapse and distant metastasis are the major causes of death in patients with colorectal cancer (Wu et al., 2017). Therefore, there is an unmet medical need for alternative efficacious treatments for patients with colorectal cancer. Among different approaches, use of plant-based drugs for colorectal cancer therapy is gaining importance.

Aegiceras corniculatum (L.) Blanco (Fig. 1) is a mangrove shrub or small tree distributed widely in coastal and estuarine areas, including India, China, New Guinea, and New South Wales, Australia. It has a long history of use in traditional Chinese medicine to treat various human ailments, including cancer, painful arthritis, and other inflammatory disorders (Deng, 2008; Hou and Deng, 2018). Different components, including triterpenes, benzoquinones, hydroquinones, flavonoids, lignans, phenolic acids, saponins, sterols, and tannins have been isolated from this plant (Kalegari et al., 2011; Vinh et al., 2017). A. corniculatum has shown anticancer activity (Ding et al., 2012), antinociceptive activity (Roome et al., 2011), antidiarrhoeal activity

* Corresponding author. Guangxi Key Laboratory of Efficacy Study on Chinese Materia Medica, Guangxi University of Chinese Medicine, Nanning, China.
** Corresponding author. Guangxi Key Laboratory of Efficacy Study on Chinese Materia Medica, Guangxi University of Chinese Medicine, Nanning, China.
E-mail addresses: yb87518@um.edu.mo (H. Luo), ewhao@163.com (E. Hao), houxt@126.com (X. Hou), dengjg@126.com (J. Deng).
[1] These authors contributed equally.

https://doi.org/10.1016/j.fct.2019.110861
Received 10 June 2019; Received in revised form 17 August 2019; Accepted 26 September 2019
Available online 01 October 2019
0278-6915/

Fig. 1. ***Aegiceras corniculatum*** **(L.) Blanco.**

(Vinh et al., 2017), anti-inflammatory activity (Roome et al., 2008), and antioxidant activity (Roome et al., 2008). Moreover, the fruit and bark extracts of *A. corniculatum* exhibit anticancer activity against gastric carcinoma, colorectal cancer, and breast cancer (Akter et al., 2014; Uddin et al., 2011). However, to the best of our knowledge, the effects and mechanisms of action of *A. corniculatum* leaf extract against colorectal cancer have not been elucidated. A large number of works should be done to explant the anticancer mechanism. In the present study, we investigated the effects of the *n*-butanol extract of *A. corniculatum* leaves (NACL) on colorectal cancer cells and its potential mechanisms of action, filled the gap in anticancer mechanism of *A. corniculatum,* hoping this study could benefit anticancer practice.

2. Materials and methods

2.1. Chemicals and reagents

RPMI 1640, McCoy's 5A, and L15 media were purchased from Wisent Bioproduct (Toronto, Canada). Foetal bovine serum (FBS), penicillin, and streptomycin were purchased from Gibco Life Technologies (NY, USA). Dimethyl sulphoxide (DMSO) was obtained from Sigma (MO, USA). [3-(4,5-dimethylthiazol-2-yl)-5-(3-carboxymethoxyphenyl)-2-(4-sulfophenyl)-2H-tetrazolium (MTS) was procured from Promega (WI, USA). The primary antibody sampler kits, *i.e.*, Apoptosis Antibody Sampler Kit, Stress and Apoptosis Antibody Sampler Kit, Pro-Apoptosis Bcl-2 Family Antibody Sampler Kit, Phospho-Akt Pathway Antibody Sampler Kit, and the responsive secondary antibodies, were obtained from Cell Signalling Technology (MA, USA). Polyvinylidene fluoride (PVDF) membrane (Immobilon-P) was purchased from Millipore (MA, USA). All other chemicals and reagents were analytical reagent grade and purchased from Sigma.

2.2. Cell lines and culture conditions

Three colon cancer cell lines, *viz.*, HT-29, SW480, and DLD-1, and human umbilical vein endothelial cells (HUVECs) were obtained from Shanghai Cell Bank (Shanghai, China) and were separately cultured in McCoy's 5A (HT-29), L15 (SW480), RPMI 1640 (DLD-1), and DMEM

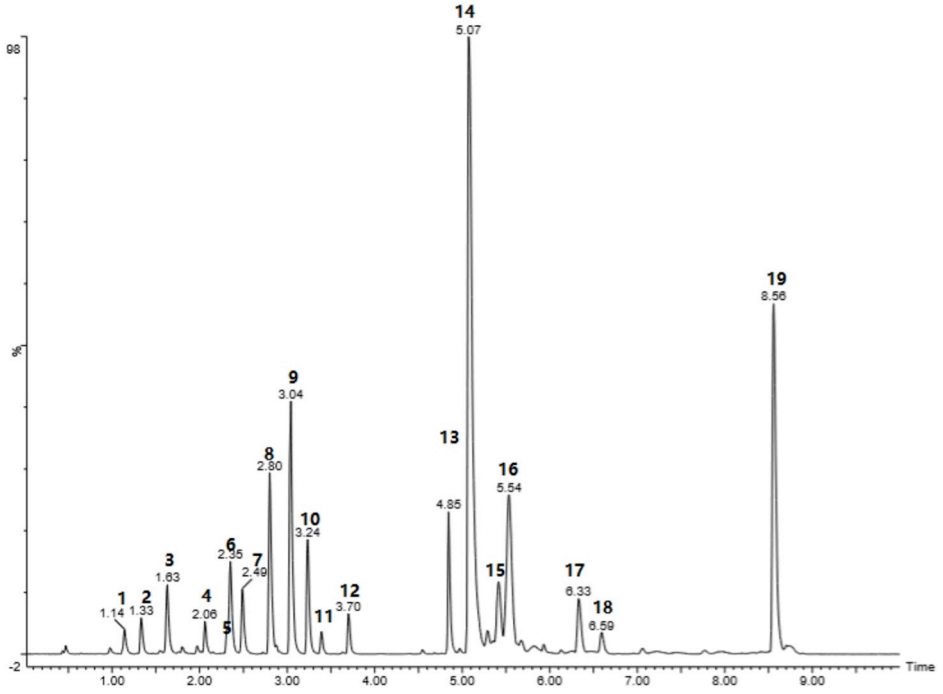

Fig. 2. Compounds identified from an *n*-butanol extract of *A. corniculatum* leaves (NACL) by UPLC-Q/TOF-MS.

(HUVECs), containing 10% FBS, 100 U/mL penicillin, and 100 μg/mL streptomycin at 37 °C and 5% CO_2.

2.3. Animals and ethics

Nude mice (male, weighing 15.0 ± 2.0 g; 4–6 weeks old) were provided by the Shanghai Laboratory Animal Center (Shanghai, China). The mice were provided food and water *ad libitum* and were allowed to acclimatise for one week before the experiments. Experimental conditions and procedures involving animals were approved by the Institutional Animal Ethics Committee (IAEC) of Guangxi Medical University (Nanning, Guangxi, China). The experiments were carried out in accordance with the Laboratory Animal Use Guidelines of IAEC. Animal handling followed the National Animal Welfare Law of China.

2.4. A. corniculatum leaf extracts

A. corniculatum leaves were collected from the seaside of Guangxi, China. The leaves were processed at the Guangxi University of Chinese Medicine to obtain *A. corniculatum* leaf extracts. Briefly, 2 kg of dried leaves were ground to a fine powder, soaked in 50 L of 95% ethanol for seven days, and then boiled and concentrated under reduced pressure. The obtained crude ethanol extract was filtered. The solution was then evaporated in vacuum to obtain the solute. The residue was suspended in deionized water at a ratio of 1:1 (m/v) and extracted successively using petroleum ether, ethyl acetate, and *n*-butanol according to the systematic solvent extraction method. The supernatant and sediment were separated by decompression filtration and the residue was re-extracted. The extracts obtained were combined and concentrated using a rotary evaporator under reduced pressure, and then were freeze-dried. The yield of each extract from crude starting materials was as follows: petroleum ether extract (PACL) 1.21%, ethyl acetate extract (EACS) 2.10%, and *n*-butanol extract (NACL) 2.19% (w/w). The extracts were stored in a freezer at −20 °C before use.

2.5. Composition analysis

NACL was analysed by liquid chromatography–mass spectrometry (LC–MS) to generate a fingerprint of phytochemicals present in the plant. One gram of NACL powder was dissolved in 1 mL of methanol, passed through a 0.22-μm microporous membrane, and analysed using an UPLC/Q-TOF-MS System. The Waters Acquity UPLC System (Waters Co., Milford, MA) equipped with a photodiode array detector (Waters Co., Milford, MA) was used. The photodiode array detector was maintained in the range of 190–400 nm. The system was controlled using Mass Lynx V4.1 software (Waters Co.). An Acquity BEH C18 column (2.1 mm i.d. × 100 mm, 1.7 μm; Waters Co.) was used for the separation. The injection volume was 3.0 μL, a gradient elution of 0.1% formic acid in water (A) and acetonitrile (B) was performed as follows: 0–4.0 min 10%–35% B (v/v), 4.0–4.5 min 35%–65% B, 4.5–7.5 min

Table 1
Relevant analytical data of compounds isolated from NACL.

Peak	RT (min)	Parent ion	MS/MS	Molecular formula	Proposed compound
1	1.14	349.0585[M-H]$^-$	96.9593	$C_{20}H_{30}O_5$	2-O-Acetyl-5-O-methylembelin (Xu et al., 2004)
	1.33	465.1434[M-H]$^-$	285.0249	$C_{21}H_{21}O_{12}$	Delphinidin-3-O-beta-glucopyranoside/isomer (Barrios et al., 2010)
			240.9977		
			138.9679		
			122.9748		
3	1.63	465.1426[M-H]$^-$	285.0251	$C_{21}H_{21}O_{12}$	Delphinidin-3-O-beta-glucopyranoside/isomer (Barrios et al., 2010)
			241.0007		
			138.9691		
			122.9748		
4	2.06	609.1438[M-H]$^-$	300.0261	$C_{27}H_{30}O_{16}$	Rutin (Xu et al., 2014)
			271.0228		
			255.0284		
5	2.32	451.1634[M-H]$^-$	225.0063	$C_{24}H_{36}O_8$	Rhodojaponin I/isomer (Zou et al., 2014)
			177.0398		
			150.9714		
			138.9702		
6	2.35	451.1625[M-H]$^-$	225.0061	$C_{24}H_{36}O_8$	Rhodojaponin I/isomer (Zou et al., 2014)
			177.0394		
			150.9704		
			138.9099		
7	2.49	564.4105[M-H]$^-$	335.0541	$C_{26}H_{28}O_{14}$	Isoschaftoside (Liu et al., 2018)
			279.2318		
8	2.80	723.4997[M-H]$^-$	723.5055	$C_{33}H_{40}O_{18}$	Kaempferol-3-rhamnoside-4″-rhamnoside-7-rhamnoside
9	3.04	836.5835[M-H]$^-$	836.5859	$C_{25}H_{42}N_7O_{17}P_3S$	Isobutyryl-coenzyme A (Liu et al., 2018)
10	3.24	949.6699[M-H]$^-$	789.5982	$C_{44}H_{70}O_{22}$	Rebaudioside C (Prakash et al., 2012)
			338.2452		
11	3.39	1062.7555[M-H]$^-$	1062.7572	$C_{51}H_{82}O_{23}$	Aegicerin saponin (Zhang et al., 2005)
12	3.70	943.4897[M-H]$^-$	781.4375	$C_{48}H_{80}O_{18}$	Protoprimulagenin saponin (Zhang et al., 2005)
			619.3854		
13	4.85	1249.6230[M-H]$^-$	1069.557	$C_{61}H_{100}O_{26}$	Sakuraso saponin/isomer (Machocho et al., 2003)
			351.1288		
			205.0713		
14	5.07	1249.6212[M-H]$^-$	1069.558	$C_{61}H_{100}O_{26}$	Sakuraso saponin/isomer (Machocho et al., 2003)
			351.1283		
			205.0710		
15	5.42	571.2885[M-H]$^-$	255.2331	$C_{32}H_{44}O_9$	Ganoderic acid H
			152.9966		
16	5.54	555.2841[M-H]$^-$	225.0066	$C_{31}H_{41}NO_8$	Acsonine
			164.9854		
17	6.33	480.3097[M-H]$^-$	255.2334	$C_{27}H_{44}O_7$	25S-Inokosterone
18	6.59	506.3249[M-H]$^-$	281.2480	$C_{29}H_{46}O_7$	Decumbesterone A
19	8.55	339.2318 [M-H]$^-$	163.1147	$C_6H_{14}O_{12}P_2$	Fructose 1,6-diphosphate

65%–70% B, 7.5–8.0 min 70%–95% B, 8.0–8.5 min 95%–100% B, and 8.5–10 min held at 100% B. The flow rate was 0.50 mL/min, and the column temperature was maintained at 30 °C. Tandem mass spectrometry (MS/MS) was performed on a Waters UPLC/Q-TOF Premier with an electrospray ionization (ESI) system (Waters MS Technologies, Manchester, UK). The ESI–MS spectra were acquired in both the negative and positive ion voltage modes. The ion source temperature was 110 °C. The capillary voltage was set to 2.5 kV for the negative mode and 3.0 kV for the positive mode. The sample cone voltage was set to 30 V. High-purity nitrogen was used as the nebulizer in the negative mode and auxiliary gases in the positive mode. The nitrogen gas flow rate was 600 L/h, temperature was 350 °C, and cone gas was set to 50 L/h. The acquisition rate was 0.1 s, with a 0.02 s inter-scan delay. Mass detection range was 50–1500 Da. Leucine enkephalinamide acetate (200 μg/L) was used as the lock mass ($[M-H]^-$ = 553.2775, $[M+H]^+$ = 555.2931).

2.6. MTS assay

Cell viability was determined by the MTS assay as described previously (Guo et al., 2017). Briefly, HT-29, SW480, DLD-1, COLO205, and HUVECs were seeded in 96-well plates and allowed to adhere overnight. The cells were then treated with the indicated concentrations of the four extracts for 24, 48, and 72 h; DMSO was used as the negative control. Subsequently, 20 μL of MTS solution was added to each well at the end points and incubated for 2 h at 37 °C. Absorbance at 490 nm was detected using a microplate reader. Cell viability rate (%) = treated group/control group × 100. The half-maximal inhibitory concentration (IC_{50}) was calculated by the Bliss method. Data are presented as the average of three independent experiments.

2.7. Colony-forming assay

HT-29, SW480, and DLD-1 cells were seeded in a six-well plate at a density of 400 cells per well. After 24 h, the cells were treated with NACL (12.5 and 25 μg/mL) or DMSO until interaction was observed between cell colonies, and the medium was replaced with fresh medium containing NACL every four days. To determine colony formation, cultures were fixed with 4.0% paraformaldehyde and stained with crystal violet. Typical images were captured and scanned. The colony formation rate (%) = number of colonies/number of plated cells × 100.

2.8. Cell cycle and apoptosis analysis

Cell cycle and apoptosis were analysed by flow cytometry (FACScan; BD Biosciences, Shanghai, China) as previously described with some modifications (Guo et al., 2017). Briefly, for cell cycle analysis, the treated cells were incubated with propidium iodide according to the manufacturer's instruction of the Cycle TEST PLUS DNA Reagent Kit (BD Pharmingen, San Diego, CA). Subsequently, 30 000 stained cells per sample were analysed by flow cytometry using FL-2A to score the DNA content of the cells. The cell population at each phase was calculated using Modfit software (Verity Software House, Topsham, ME). For the apoptosis analysis, apoptotic cells were detected using the Annexin V-FITC Apoptosis Detection kit I (BD Pharmingen), following the manufacturer's protocols. Briefly, the treated cells were trypsinised, washed, collected, suspended in binding buffer, and stained with Annexin V-FITC and PI for 15 min at 25 °C in the dark. At the end, approximately 30 000 cells per sample were collected and analysed by flow cytometry. The experiments were conducted in triplicate, and the results are presented as the mean of three experiments.

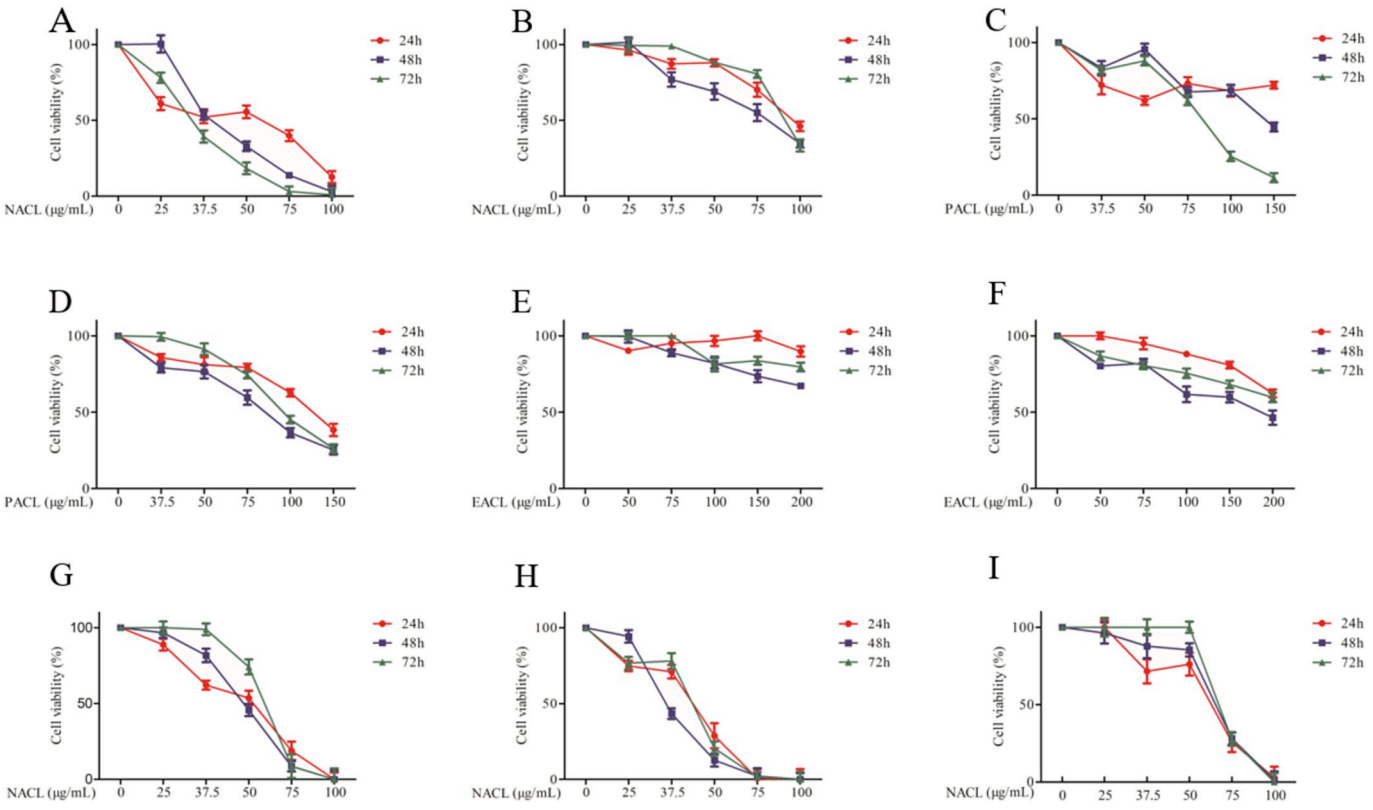

Fig. 3. *A. corniculatum* leaf extracts inhibited the viability and colony formation of colorectal cancer and HUVECs. Cytotoxicity of NACL for (A) HT-29 cells; (B) SW480 cells. Cytotoxicity of petroleum ether extract (PACL) for (C) HT-29 cells; (D) SW480. Cytotoxicity of ethyl acetate extract (EACL) for (E) HT-29 cells; (F) SW480 cells. Cytotoxicity of NACL for (G) DLD-1 cells; (h) COLO205 cells; (I) HUVECs. Similar results were obtained in 3 independent experiments. Data areexpressed as mean ± SD.

Table 2
IC50 values of NACL for cancer cells (mean ± SD; μg/mL).

Time (h)	HT-29	SW480	DLD-1	COLO205	DU145	PC3
24	42.30 ± 0.46	61.28 ± 0.68	46.48 ± 0.70	39.08 ± 0.85	80.80 ± 0.72	46.31 ± 0.61
48	43.43 ± 0.86	40.69 ± 0.61	48.26 ± 1.14	36.78 ± 1.41	92.56 ± 1.85	45.80 ± 0.73
72	34.01 ± 0.89	37.90 ± 1.08	56.72 ± 2.02	39.52 ± 0.93	85.82 ± 2.11	50.69 ± 0.72
Time (h)	**SGC-7901**	**SKOV3–S**	**Tca-8113**	**MDA-MB-231**	**A2780**	**HeLa**
24	58.01 ± 0.53	45.08 ± 0.92	56.91 ± 0.60	37.24 ± 0.74	118.22 ± 0.53	98.84 ± 1.57
48	61.03 ± 0.94	47.22 ± 1.42	40.46 ± 0.78	49.43 ± 1.05	94.50 ± 0.81	93.58 ± 1.80
72	50.82 ± 0.67	52.18 ± 1.48	53.94 ± 1.74	35.40 ± 0.62	58.80 ± 0.49	96.38 ± 1.62
Time (h)	**HepG2**	**PANC-1**	**SMMC-7721**	**Bel-7402**	**MCF-7**	**HUVEC**
24	38.38 ± 0.53	78.18 ± 0.46	41.51 ± 0.56	65.51 ± 0.48	42.56 ± 0.47	57.18 ± 0.85
48	53.97 ± 0.92	78.58 ± 0.62	59.15 ± 2.00	80.37 ± 0.95	38.99 ± 0.51	61.20 ± 0.97
72	52.56 ± 1.32	70.10 ± 0.99	60.73 ± 1.84	67.88 ± 0.65	46.49 ± 0.54	70.86 ± 9.64

2.9. Western blotting

Western blotting was conducted as described previously (Guo et al., 2017). Total protein was extracted, and the protein concentration was determined using the BCA™ Protein Assay Reagent kit (Pierce Chemical Co., Rockford, IL). The protein samples were separated by sodium dodecyl sulphate–polyacrylamide gel electrophoresis (SDS–PAGE), and then transferred onto polyvinylidene fluoride (PVDF) membranes. After blocking with 5% non-fat milk in tris-buffered saline–Tween (TBST) for 1 h, the blots with primary antibodies (1:1000) were incubated overnight at 4 °C. After washing three times with TBST, the blots were incubated with the secondary antibody conjugated with peroxidase for 1 h and an enhanced chemiluminescence detection system (Sage Creation Science Co, Beijing, China) was used for detection. Glyceraldehyde 3-phosphate dehydrogenase (GAPDH) or β-actin were used as a loading control.

2.10. Tumour xenografts in nude mice and drug treatments

Fifty 4–6-weeks-old mice were housed under specific pathogen-free conditions. Two million colon cancer cells (HT-29) were subcutaneously injected into the right flank of each mouse (day 0). When the primary tumours reached a mean volume of approximately 50 mm^3, the mice carrying tumour xenografts were randomly divided into three groups ($n = 10$ per group) and subjected to treatments. The mice were orally treated with NACL (25 mg/kg) once daily for 18 consecutive days. 5-Fluorouracil (5-FU) (20 mg/kg), used as the reference positive control, was administered intraperitoneally twice a week. The body weight and tumour size of the mice were monitored every three days, and the tumour weight was determined at the end of the study. Volume of tumour = (length × [width]^2)/2. The mice were sacrificed by CO_2 asphyxiation, and the tumours were removed and stored at −80 °C until further analysis.

2.11. Statistical analysis

The data are expressed as mean ± SD of at least three replicates per group. The data were analysed by one-way analysis of variance with Tukey's test or an unpaired *t*-test using SPSS (version 17.0; IBM Corp., Armonk, NY). Differences were considered statistically significant at $p < 0.05$ and $p < 0.01$.

3. Results

3.1. Phytochemical analysis of NACL

The phytochemicals in NACL were analysed by UPLC-Q/TOF-MS. Fig. 2 shows the base peak chromatogram of NACL obtained by UPLC-MS. All compounds were characterised by interpreting their mass spectra obtained by MS/MS and were further compared with published data. The sixteen compounds identified, including flavonoid glycosides, benzoquinones, saponins, diphosphates, tetracyclic diterpenoids, and steroids, are summarised in Table 1.

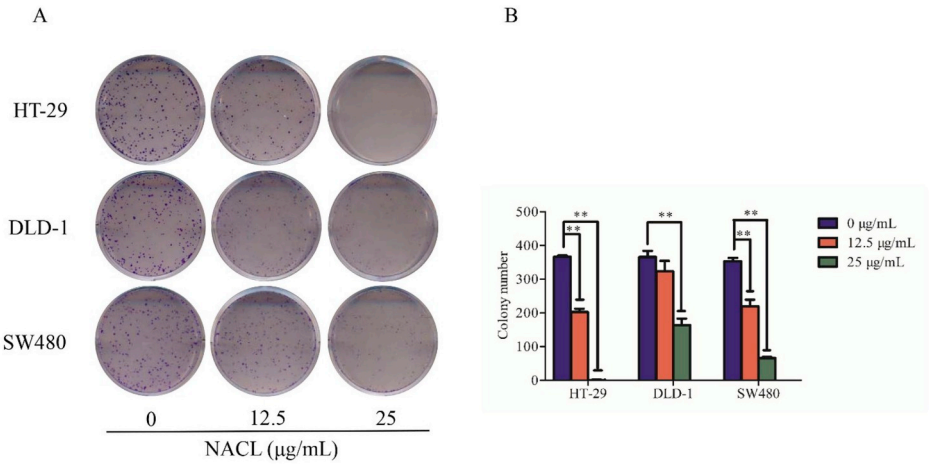

Fig. 4. Clonogenic growth potential of colorectal cancer cells treated with NACL. Similar results were obtained in 3 independent experiments. Data are expressed as mean ± SD and percent of the control. **, $p < 0.01$.

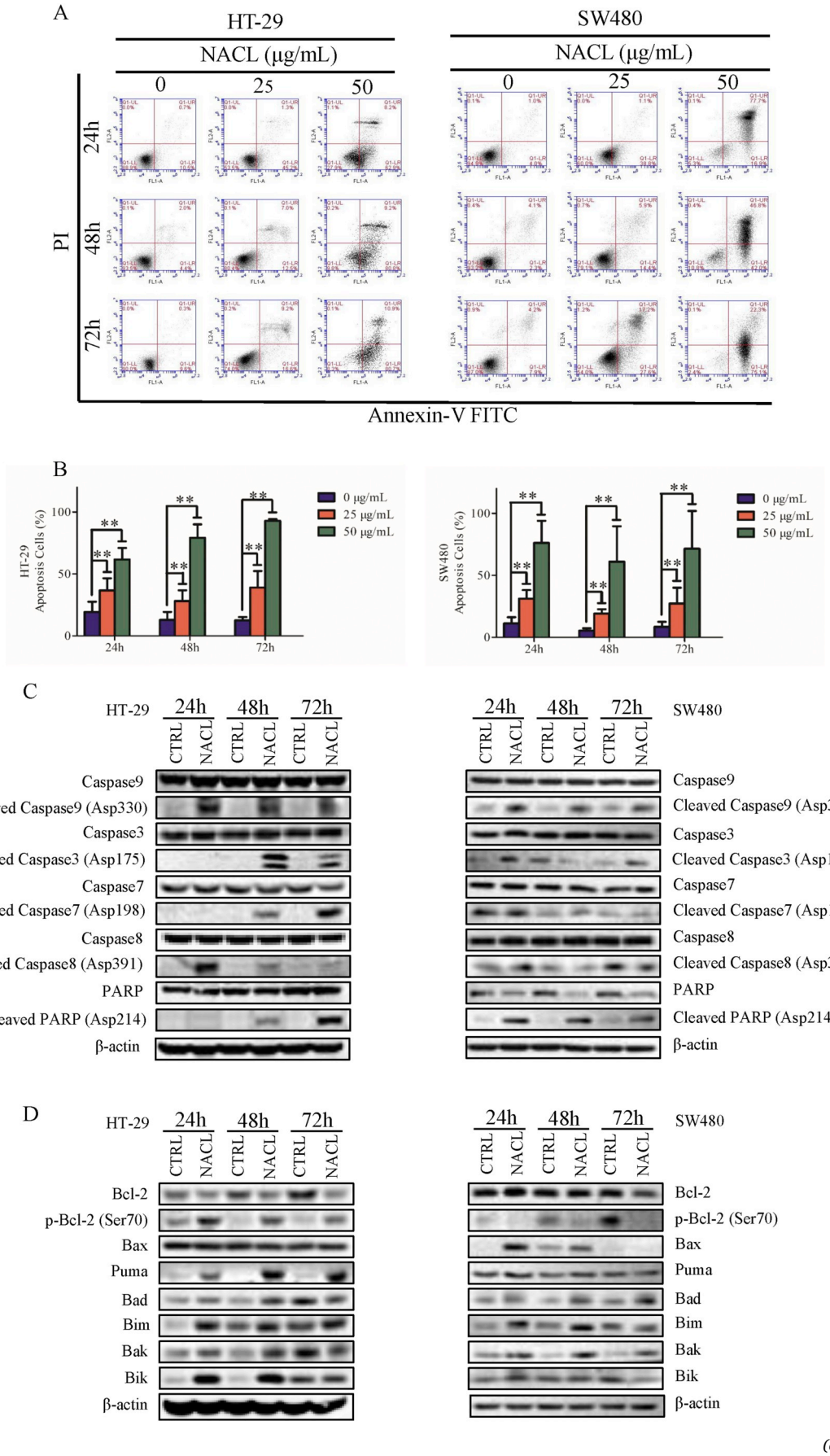

(caption on next page)

Fig. 5. Induction of apoptosis by NACL in colorectal cancer cells. (A) Annexin V-negative/PI-negative cells (regarded as normal) are in the lower left quadrant and Annexin V-positive/PI-negative cells are early apoptotic cells in the lower right quadrant. Late apoptotic Annexin V-positive/PI-positive cells are in the upper right quadrant, and necrotic Annexin V-negative/PI-positive cells are in the upper left quadrant. (B) Quantitative representation of apoptotic cells in panel A. *, $p < 0.05$; **, $p < 0.01$. (C) Caspases, the central regulators of apoptosis, were detected by western blotting in colorectal cancer cells. (D) Bcl-2 family proteins were detected by western blotting in colorectal cancer cells. (E)The relative density of proteins in the figure C. (F) The relative density of proteins in the figure D. Similar results were obtained in 3 independent experiments. Data are expressed as mean ± SD and percent of the control. **, $p < 0.01$.

3.2. *A. corniculatum* leaf extracts inhibited the viability and colony formation of colorectal cancer

To investigate the effects of *A. corniculatum* on colorectal cancer cell proliferation, HT-29 and SW480 cells were treated with PACL, EACL, and NACL at the indicated concentrations for 24, 48, and 72 h. Cell viability was determined by the MTS assay; HUVECs were used as the normal control. As shown in Fig. 3, the NACL inhibited cell growth in a dose-dependent manner, and it was more potent in inhibiting colorectal cancer cell proliferation than the other two extracts. The anticancer effects of NACL were also observed in the other colorectal cancer cell lines, *viz.*, DLD-1 and COLO205 (Fig. 3). Inhibitory activity of NACL on human umbilical vein endothelial cells (HUVECs) was observed only at the higher concentrations. The IC_{50} value of NACL is summarised in Fig. 3J and Table 2. It ranged from 34.01 to 61.28 μg/mL for colorectal cancer cell lines. Furthermore, NACL also exhibited significant anticancer activity against prostate, breast, liver, ovarian, cervical, and gastric cancers.

In addition, a clonogenic assay was performed to further validate the anti-proliferative effect of NACL on colorectal cancer cells. The colony-forming ability of HT-29, SW480, and DLD-1 cells was significantly suppressed in a dose-dependent manner after treatment with NACL (Fig. 4).

3.3. NACL induced apoptosis in colorectal cancer cells

To determine the primary cause triggering cell death, the pro-apoptotic effect of NACL on colorectal cancer cells was examined by flow cytometry with Annexin V/PI staining. After treating HT-29 and SW480 cells with NACL for 24, 48, and 72 h, the population of apoptotic cells in each cell type increased in a dose-dependent manner (Fig. 5A and B), ranging from 12.55% to 92.95% in HT-29 cells and from 8.46% to 71.43% in SW480 cells treated with 50 μg/mL of NACL.

To further explore the molecular mechanisms underlying NACL-induced apoptosis of colorectal cancer cells, the expression of a panel of proteins involved in cellular apoptosis was determined by western blotting. Cleavage of Caspase-9 and -8, and of poly(ADP-ribose) polymerase (PARP) was significantly induced after treatment with NACL for 24 h, in both HT-29 and SW480 cells, suggesting both intrinsic (caspase-9) and extrinsic (caspase-8) apoptosis pathways are activated, leading to the cleavage of caspase-3 and -7 and their activation (Fig. 5C). These changes were more drastic in HT-29 cells than in SW480 cells, which was consistent with their respective IC_{50} values with NACL.

We continued to examine BCL-2 family proteins in cells treated with NACL, and found that BIM, PUMA, BIK, BAK pro-death proteins, and phosphor-BCL-2 (inhibiting its anti-death function) were increased by NACL in HT-29 after treatment for 24 h, while BIM, BAK, BAX, and phospho-BCL-2 were increased in SW480 (Fig. 5D). The more profound changes in pro-death proteins in HT-29 cells were also consistent with the activation of caspases in these cells shown in Fig. 5C.

3.4. NACL induced cell cycle arrest in colorectal cancer cells

After treatment with NACL for 24, 48, and 72 h, cell cycle distribution was measured in HT-29 and SW480 cells by flow cytometry. As shown in Fig. 6A, the G0/G1 phase cell population was significantly increased after treatment of HT-29 cells with NACL from 24 to 72 h, whereas only minor changes in cell cycle distribution were observed in SW480 cells (Fig. 6B).

To explore the mechanism underlying cell cycle arrest, some cell cycle-related proteins and checkpoint molecules were analysed by western blotting (Fig. 6C). The results showed that the expression of p21, a CDK inhibitor, and the phosphorylation of Chk1, Chk2, and Rb cell cycle checkpoint molecules increased, whereas the level of cell cycle regulators Cyclin D3, Cyclin D1, CDK2, CDK4, and CDK6 decreased in NACL-treated HT-29 cells. On the contrary, the expression of p21 and p27 and phosphorylation of Chk2 were increased, and the phosphorylation of Chk1 was decreased by NACL in SW480 cells.

To further explore underlying molecular mechanisms, we investigated the Forkhead signalling pathway. With western blot analysis, we found that NACL treatment significantly upregulated the total FoxO1 and FoxO3a and the phosphorylation of FoxO1 (Ser256), FoxO3 (Ser253), FoxO1/FoxO3a and FoxO1/FoxO3a/FoxO4 in HT-29 cells, but only the total FoxO3a and the phosphorylation of FoxO3a (Ser253) and FoxO1/FoxO3a/FoxO4 in SW480 cells (Fig. 6C). The increase in FOX03a may contribute to the induction of BIM protein shown in Fig. 6D.

3.5. NACL suppressed the growth of HT-29 xenografts in nude mice

After studying the effects and mechanism of action of NACL *in vitro*, we proceeded to investigate NACL's anti-tumour activity *in vivo*. To that end, we used a HT-29 xenograft model in nude mice. After treatment with NACL and 5-FU (used as a positive control), the tumour volumes and weight of the treatment groups were shown to be smaller and lighter than those of the negative control group, and the difference in tumour volume between the negative control and treated groups became more significant with increasing treatment time (Fig. 7A, B, C). More specifically, the tumour volume in the NACL group (25 mg/kg/day) was diminished to approximately 62.48% compared to that of the negative control group. In addition, no significant loss of body weight was observed in either group, suggesting that NACL is safe at the used treatment dosage (Fig. 7C).

4. Discussion

As a marine medicinal plant, the leaf of *A. corniculatum*, a species of shrub or tree mangrove, has long been used in China to treat various human ailments. Our previous study with NACL showed that it exerts anti-prostate cancer efficacy by inducing apoptosis and inhibiting metastasis (Luo et al., 2018), and the ethyl acetate extract (EACL) of *A. corniculatum* stems exhibits an inhibitory effect on the proliferation of nineteen tumour cell lines, including colorectal cancer, prostate cancer, breast cancer, ovarian cancer and so on (Tan et al., 2018).

In this study, we focused on studying NACL to understand its components and, more importantly, the molecular mechanism of its anti-tumour activities, especially in colorectal cancer. This is the first study of its kind to elucidate and report the molecular functions of the extract in colorectal cancer.

Using HPLC and NMR to analyse the ingredients of NACL, we discovered that it contains multiple components, including flavonoid glycosides, phenolic glycosides, saponins, polysaccharides, and steroids, which is consistent with published data (Dun et al., 2015; Xu et al., 2014; Zou et al., 2014). Embelin, previously identified from the PACL of *A. corniculatum*, has been shown to have a potent anticancer effect. It has also been reported that flavonoid glycosides are highly

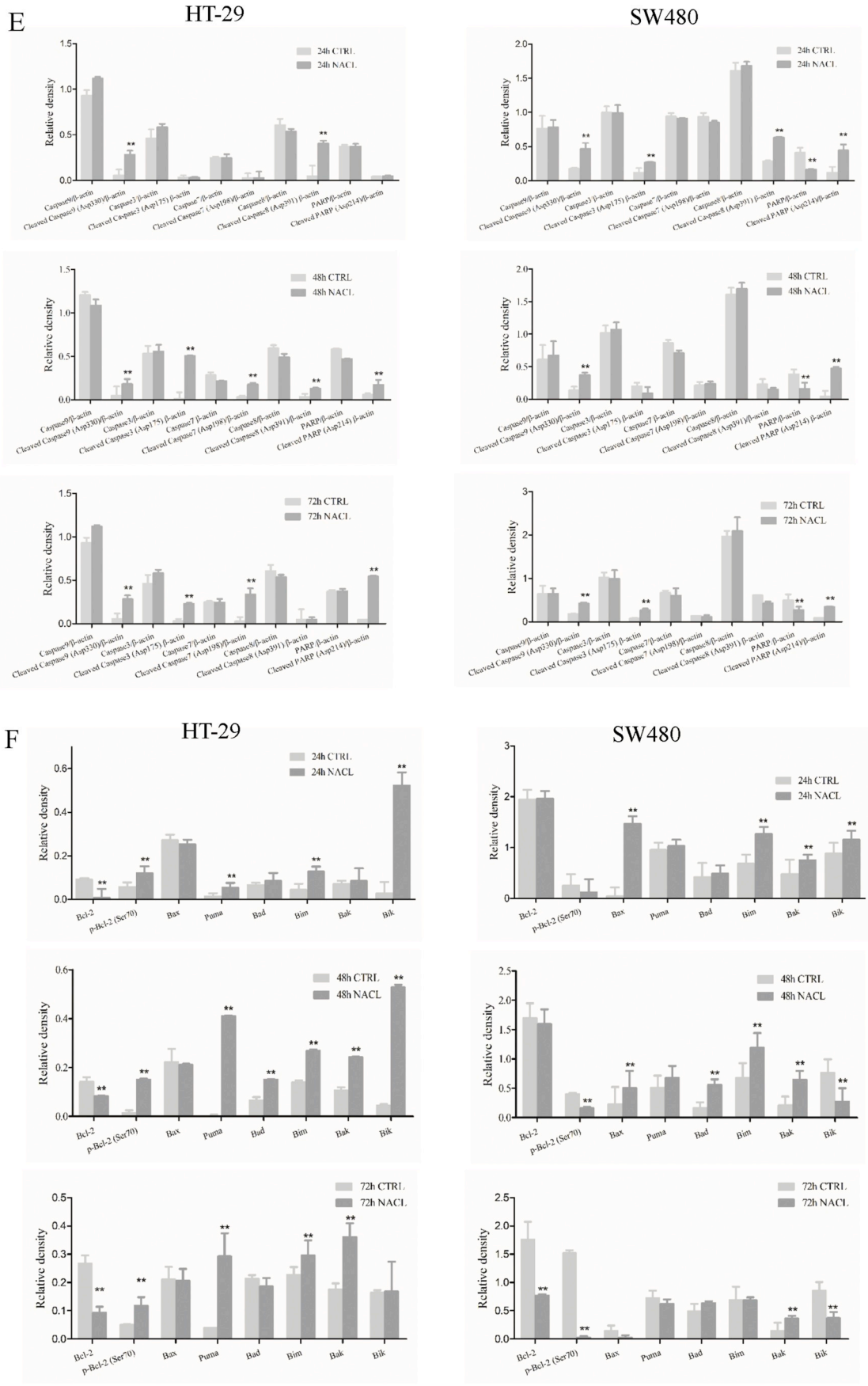

Fig. 5. (*continued*)

active compounds, with a wide range of pharmacological applications, particularly as anticancer agents.

Using NACL, we demonstrated that it can inhibit the growth of colorectal cancer cells, reducing their viability, proliferation, and colony formation, at least in part by regulating the cell cycle and apoptosis pathway. Three members (FoxO1, FoxO4, and FoxO3a) of the Forkhead family have sequence similarity to the nematode ortholog DAF-16, which mediates signalling through a pathway involving IGFR1,

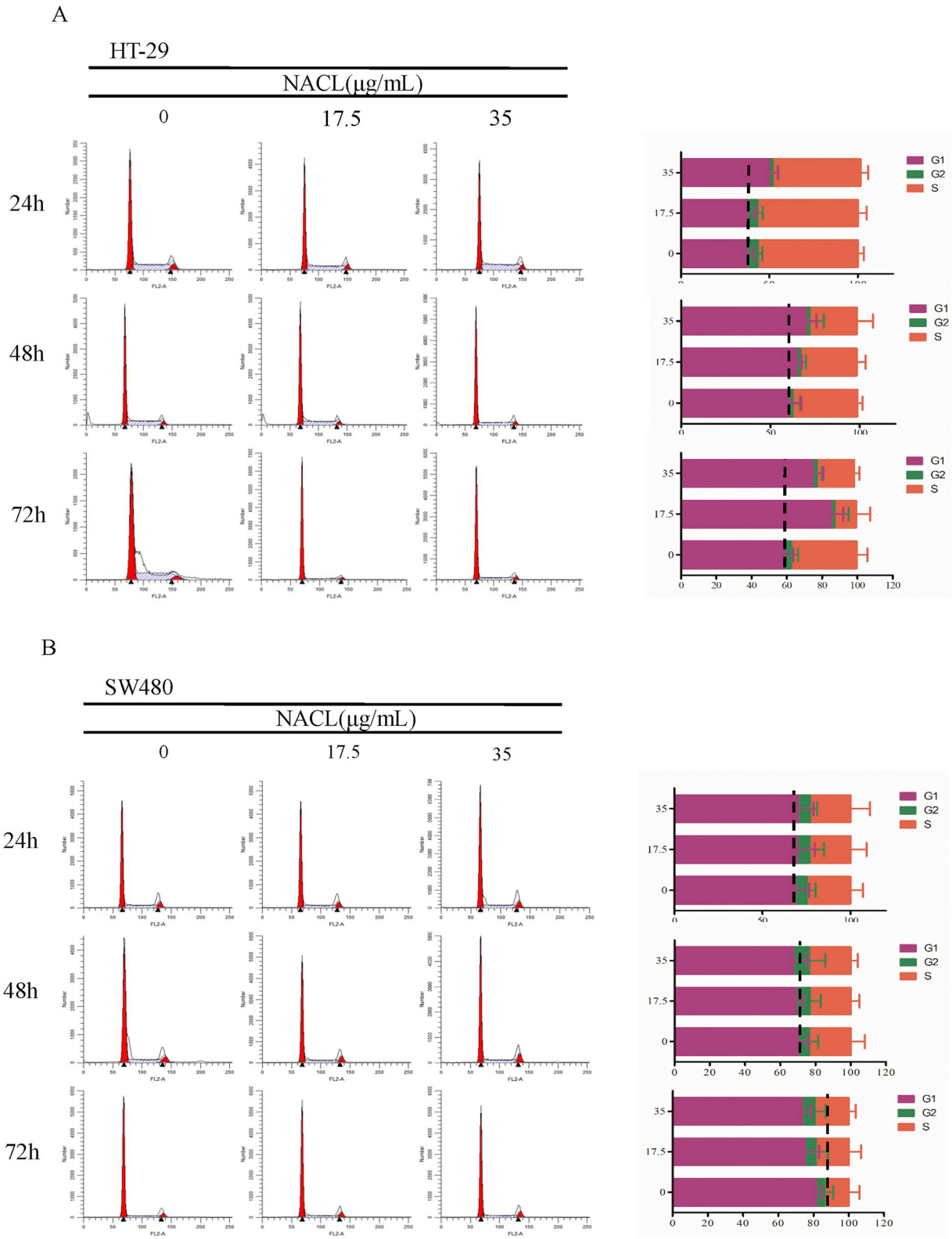

Fig. 6. NACL-induced cell cycle arrest in colorectal cancer cells. (A) HT-29 cells were treated with 17.5 and 35 μg/mL NACL for 24, 48, and 72 h and the cell cycle assays were conducted by flow cytometry. (B) SW480 cells were treated with 17.5 and 35 μg/mL NACL for 24, 48, and 72 h and the cell cycle assays were conducted by flow cytometry. (C) Expression of cell cycle-related proteins was determined by western blotting. (D) The relative density of proteins in the figure C. Similar results were obtained in 3 independent experiments. Data are expressed as mean ± SD and percent of the control. **, $p < 0.01$.

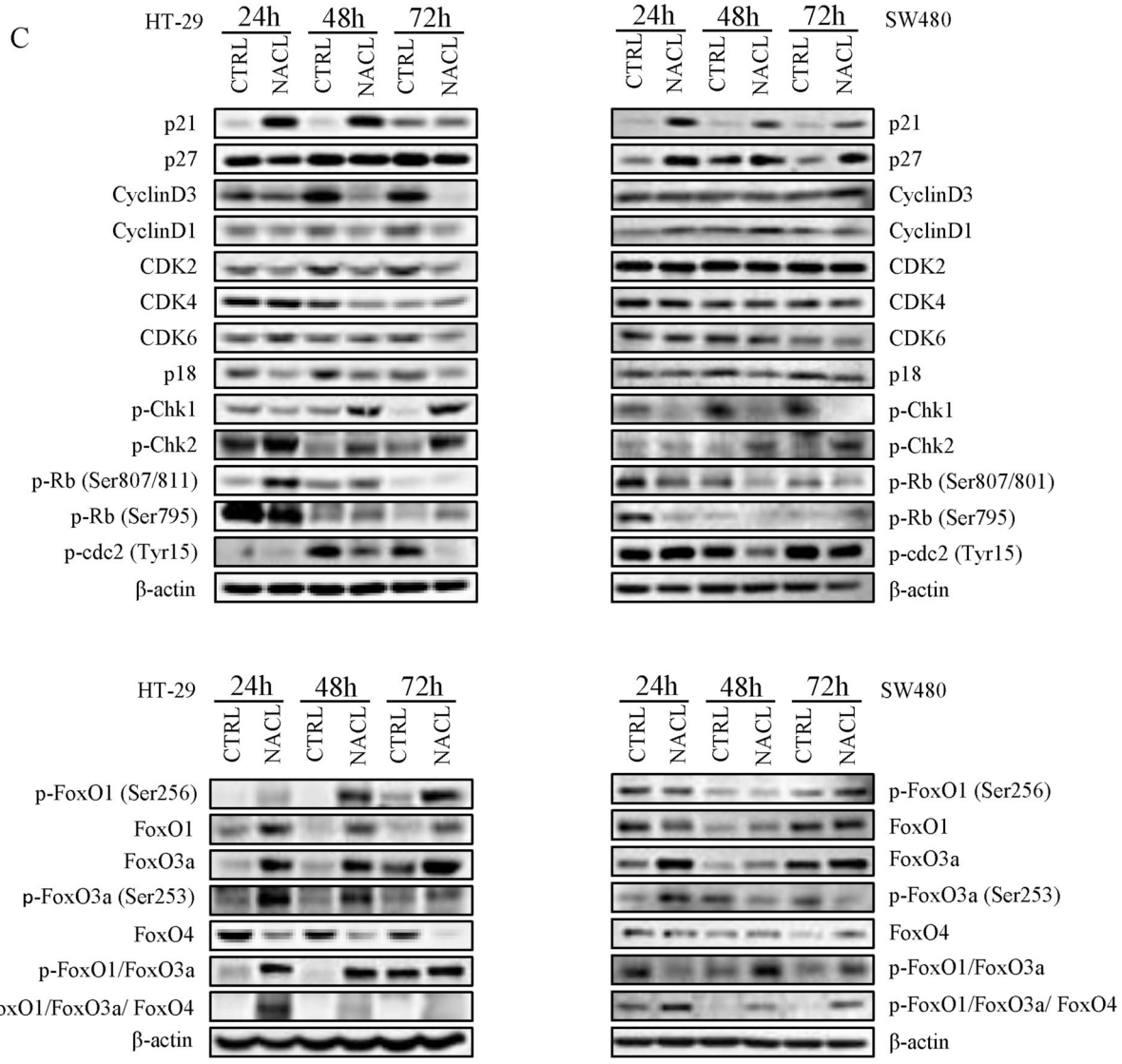

Fig. 6. (*continued*)

PI3K, and Akt. Active Forkhead members act as tumour suppressors by promoting cell cycle arrest and apoptosis (Seoane et al., 2004). Forkhead transcription factors are involved in the TGF-β-mediated upregulation of p21, a process negatively regulated through PI3K. Further analysis of the FoxO family revealed that NACL induces FoxO1 and Fox03a in HT-29 cells, which may trigger intrinsic and extrinsic apoptosis signals. As shown in Fig. 7, NACL potentially induces apoptosis in HT-29 cells by inducing the Bcl-2 family proteins, such as BIM, then activating caspase-3 and -7. The final executioner of cell apoptosis is caspase-3/-7, which was also shown in this study to be activated by caspase-8 and -9.

The potential mechanism of action of NACL is by inducing cell cycle arrest, possibly through FoxO activating transcript cell cycle kinase inhibitor p21, leading to the inhibition of CDK4/6 and cyclin D1. Then the Rb protein is inhibited by CDK4/6 and cyclin D1. The more profound changes in cell cycle regulation and pro-death proteins in HT-29 cells than in SW480 cells are consistent with their higher sensitivity to NACL.

The xenograft model in nude mice confirmed again that NACL can inhibit tumour growth *in vivo*. However, at the higher concentration of 50 mg/kg, it showed some toxicity, resulting in decreased body weight. The NACL used in the present study was a crude extract, and in the future, we will try to purify it, improving its efficacy and reducing its side effects or toxicity. Additionally, it can be combined with other drugs, such as 5-FU, that presently are the standard of care, to enhance their effect in colorectal cancer patients.

5. Conclusion

Traditional Chinese medicines show enhanced efficacy and immunomodulatory functions through their multi-component, multi-target, and multi-channel effects along with reduced toxicity compared to conventional synthetic drugs. Through these results of the role of NACL in the regulation of cellular pathways, there is an advancement from just applying the crude extract to an understanding of its molecular mechanisms. Thus, by identifying the active components of traditional Chinese medicines, new candidate drugs can be developed for cancer therapy.

Author contributions

H.L. performed most of the experiments, analysed the data and wrote the article; D.T., X.F., X.Y. and C.H. performed MTS test and collected the medicine; W.W., G.B., C.C. and Y.H. performed the chemical analyses; H.L., E.H., X.H., J.D. and Y.W. designed the project; J.L. and Z.D. provided reagents. All authors reviewed and approved the manuscript.

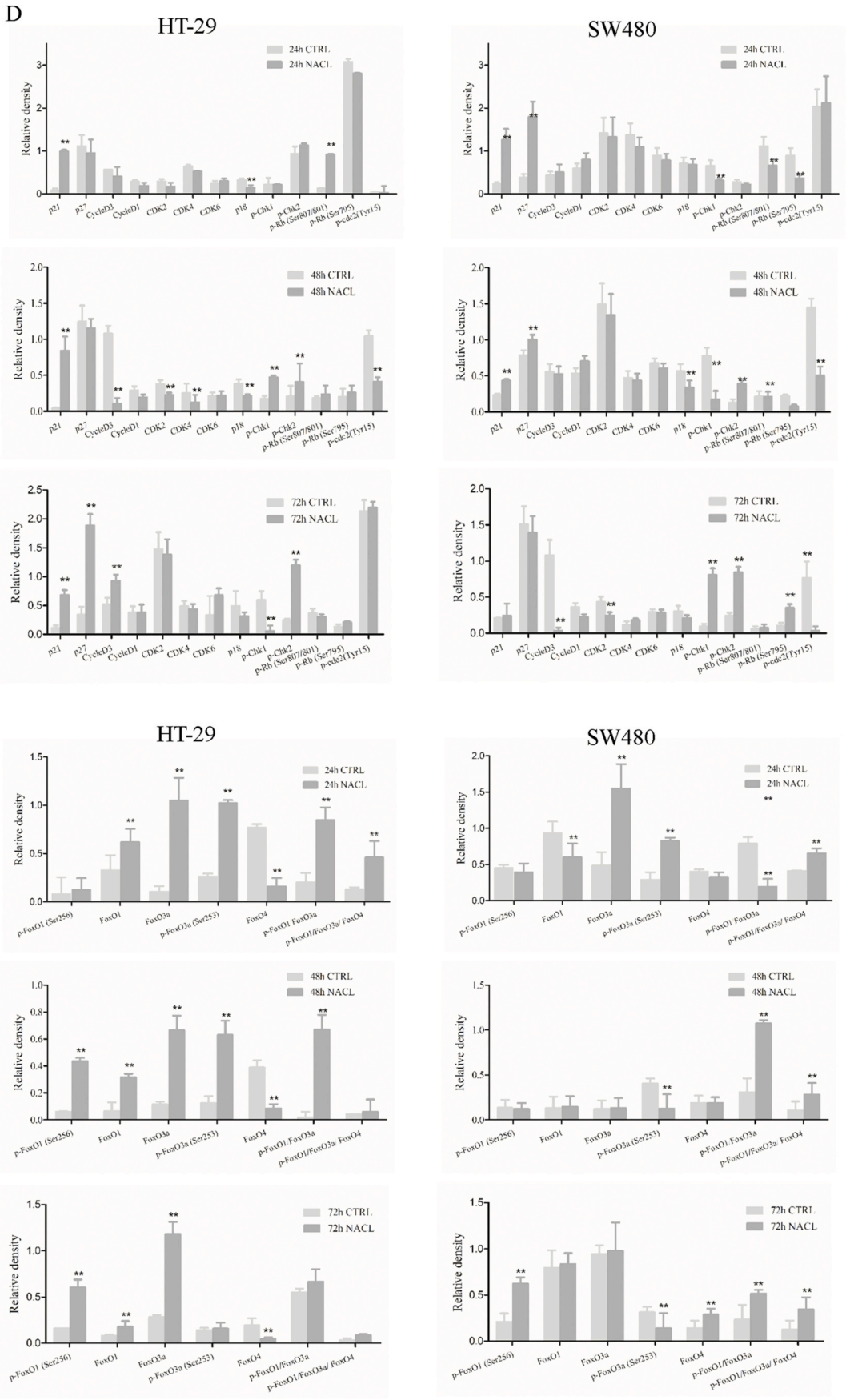

Fig. 6. (*continued*)

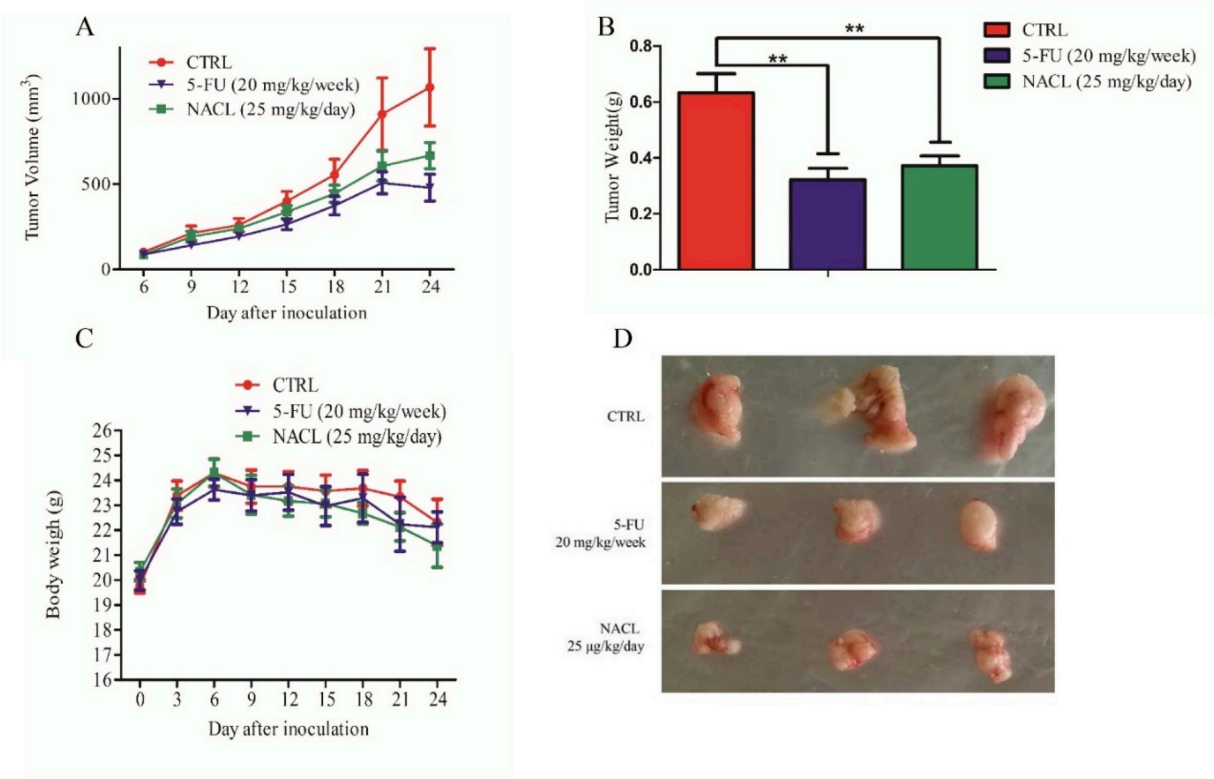

Fig. 7. NACL inhibited tumour growth in xenograft nude mouse model. Nude mice (n = 10 mice per group) were implanted with 2×10^6 HT-29 cells by subcutaneous injection, and then treated with 25 mg/kg NACL via oral administration for 18 consecutive days from day 5 on, when tumour cells were implanted successfully *in vivo*. Fluorouracil (5-FU, 20 mg/kg) was used as the positive control for reference; it was administered by intraperitoneal injection once a week. (A) Tumour volume in the treatment, positive control, and control group. Data are expressed as mean ± SD. (B) Tumour weight in the control, positive control, and treatment group. (C) Body weight was assessed in the mice every three days. (D) Tumours were harvested on day 24. Similar results were obtained in 3 independent experiments. Data are expressed as mean ± SD and percent of the control. **, $p < 0.01$.

Funding

The study was supported by the Guangxi Scientific Research and Technology Development Plan Project (No. GKH15104001-11), Guangxi Science and Technology Plan Projects (No. GKAD17195025), and Guangxi Key Laboratory Construction Project (No.17-259-20).

Declaration of competing interest

The authors declare that they have no known competing financial interests or personal relationships that could have appeared to influence the work reported in this paper.

Acknowledgements

We thank Jing Deng (Harvard Medical School), Dr. Jianbo Xiao (University of Macau), Dr. Jian Zhang (Southern University of Science and Technology), and Dr. Yu Lu (Southern University of Science and Technology) for valuable discussions.

Appendix A. Supplementary data

Supplementary data to this article can be found online at https://doi.org/10.1016/j.fct.2019.110861.

References

Akter, R., Uddin, S.J., Grice, I.D., Tiralongo, E., 2014. Cytotoxic activity screening of Bangladeshi medicinal plant extracts. J. Nat. Med. 68, 246–252.

Alkema, L., Chou, D., Hogan, D., Zhang, S., Moller, A.B., Gemmill, A., et al., 2016. Global, regional, and national levels and trends in maternal mortality between 1990 and 2015 with scenario-based projections to 2030: a systematic analysis by the UN Maternal Mortality Estimation Inter-Agency Group. Lancet 387, 462–474.

Barrios, J., Cordero, C.P., Aristizabal, F., Heredia, F.J., Morales, A.L., Osorio, C., 2010. Chemical analysis and screening as anticancer agent of anthocyanin-rich extract from Uva Caimarona (Pourouma cecropiifolia Mart.) fruit. J. Agric. Food Chem. 58, 2100–2110.

Chen, W., Zheng, R., Baade, P.D., Zhang, S., Zeng, H., Bray, F., et al., 2016. Cancer statistics in China, 2015. CA Cancer J. Clin. 66, 115–132.

Deng, J.G., 2008. Guangxi Marine Phytomedicines. Guangxi, Nanning. Guangxi Science and Technology Press, Nanning, Guangxi, China.

Ding, L., Dahse, H.M., Hertweck, C., 2012. Cytotoxic alkaloids from Fusarium incarnatum associated with the mangrove tree Aegiceras corniculatum. J. Nat. Prod. 75, 617–621.

Dun, J.L., Zhao, Y.W., Zheng, G.S., Zhu, H., Ruan, L.J., Wang, W.F., et al., 2015. PapR6, a putative atypical response regulator, functions as a pathway-specific activator of pristinamycin II biosynthesis in Streptomyces pristinaespiralis. J. Bacteriol. 197, 441–450.

Guo, H., Luo, H., Yuan, H., Xia, Y., Shu, P., Huang, X., et al., 2017. Litchi seed extracts diminish prostate cancer progression via induction of apoptosis and attenuation of EMT through Akt/GSK-3β signaling. Sci. Rep. 7, 41656. https://doi.org/10.1038/srep41656.

Hou, X.T., Deng, J.G., 2018. Marine chemistry of Chinese materia medica. In: Guangxi Nanning: Guangxi Science and Technology Press, Nanning, Guangxi, China.

Kalegari, M., Miguel, M.D., Dias, J.F.G., Lordello, A.L.L., Lima, C.P., Miyazaki, C.M.S., et al., 2011. Phytochemical constituents and preliminary toxicity evaluation of leaves from Rourea induta Planch. (Connaraceae). Braz. J. Pharm Sci. 47, 635–642.

Kuipers, E.J., Grady, W.M., Lieberman, D., Seufferlein, T., Sung, J.J., Boelens, P.G., et al., 2015. Colorectal cancer. Nat. Rev. Dis. Primers 1, 15065.

Liu, X.C., Yan, W.Y., Wang, X., Fan, X.Y., Lü, T., Wang, C.Y., et al., 2018. Simultaneous determination of main ingredients of Abri Herba and Abri Mollis Herba in rat urine and bile by HPLC-MS/MS and its application to a comparative study of their excretion kinetics after oral administration. Chin. J. Pharm. Anal. 38, 406–417.

Luo, H., Hao, E.W., Tan, D.C., Du, Z.C., Feng, X.H., Hou, X.T., et al., 2018. Anti-prostate cancer activities of N-butanol extract of Aegiceras corniculatum leaves in vitro. J. Chin. Med. Mater. 8, 1977–1981.

Machocho, A.K., Kiprono, P.C., Grinberg, S., Bittner, S., 2003. Pentacyclic triterpenoids from Embelia schimperi. Phytochemistry 62, 573–577.

Prakash, I., Campbell, M., Chaturvedula, V.S., 2012. Catalytic hydrogenation of the sweet principles of Stevia rebaudiana, Rebaudioside B, Rebaudioside C, and Rebaudioside D and sensory evaluation of their reduced derivatives. Int. J. Mol. Sci. 13,

15126–15136.
Roome, T., Dar, A., Ali, S., Naqvi, S., Choudhary, M.I., 2008. A study on antioxidant, free radical scavenging, anti-inflammatory and hepatoprotective actions of Aegiceras corniculatum (stem) extracts. J. Ethnopharmacol. 118, 514–521.
Roome, T., Dar, A., Naqvi, S., Choudhary, M.I., 2011. Evaluation of antinociceptive effect of Aegiceras corniculatum stems extracts and its possible mechanism of action in rodents. J. Ethnopharmacol. 135, 351–358.
Seoane, J., Le, H.V., Shen, L., Anderson, S.A., Massagué, J., 2004. Integration of Smad and Forkhead pathways in the control of neuroepithelial and glioblastoma cell proliferation. Cell 117, 211–223.
Siegel, R.L., Miller, K.D., Fedewa, S.A., Ahnen, D.J., Meester, R.G.S., Barzi, A., et al., 2017a. Colorectal cancer statistics, 2017. CA Cancer J. Clin. 67, 177–193.
Siegel, R.L., Miller, K.D., Jemal, A., 2017b. Cancer statistics, 2017. CA Cancer J. Clin. 67, 7–30.
Tan, D.C., Luo, H., Deng, J.G., Hao, E.W., Yi, X.X., Feng, X.H., et al., 2018. Screening antitumor activity of four mangrove plants in Guangxi coastal area. Guihaia 38, 1267–1276.
Torre, L.A., Bray, F., Siegel, R.L., Ferlay, J., Lortet-Tieulent, J., Jemal, A., 2015. Global cancer statistics, 2012. CA Cancer J. Clin. 65, 69–90.
Uddin, S.J., Grice, I.D., Tiralongo, E., 2011. Cytotoxic effects of Bangladeshi medicinal plant extracts. Evid. Based Complement. Alternat. Med. 2011, 578092. https://doi.org/10.1093/ecam/nep111.
Vinh, L.B., Nguyet, N., Yang, S.Y., Kim, J.H., Thanh, N.V., Cuong, N.X., et al., 2017. Cytotoxic triterpene saponins from the mangrove Aegiceras corniculatum. Nat. Prod. Res. 16, 1–7.
Wu, X.Y., Fang, J., Wang, Z.J., Chen, C., Liu, J.Y., Wu, G.N., et al., 2017. Identification of RING-box 2 as a potential target for combating colorectal cancer growth and metastasis. Am. J. Cancer Res. 7, 1238–1251.
Xu, M., Deng, Z., Li, M., Li, J., Fu, H., Proksch, P., et al., 2004. Chemical constituents from the mangrove plant, Aegiceras corniculatum. J. Nat. Prod. 67, 762–766.
Xu, W., Fu, Z.Q., Lin, J., Huang, X.C., Yu, H.M., Huang, Z.H., et al., 2014. Rapid simultaneous determination of ten major flavonoids in Tetrastigma hemsleyanum by UPLC-MS/MS. Acta Pharm. Sin. 49, 1711–1717.
Zhang, D., Zhang, S., Wu, J., Huang, J.S., Tian, Y., Xu, L.R., 2005. Pentacyclic triterpenes from Aegiceras corniculatum. Nat. Prod. Res. Dev. 17, 306–308.
Zou, H.Y., Luo, J., Xu, D.R., Kong, L.Y., 2014. Tandem solid-phase extraction followed by HPLC-ESI/QTOF/MS/MS for rapid screening and structural identification of trace diterpenoids in flowers of Rhododendron molle. Phytochem. Anal. 25, 255–265.